Photolysis of Astrophysically Relevant Acrylonitrile: A Matrix Experimental Study

ARTICLE *in* THE JOURNAL OF PHYSICAL CHEMISTRY A · MARCH 2014

Impact Factor: 2.69 · DOI: 10.1021/jp412481s · Source: PubMed

4 AUTHORS, INCLUDING:

Abdelkrim Toumi
Aix-Marseille Université
3 PUBLICATIONS **4** CITATIONS
SEE PROFILE

Isabelle Couturier-Tamburelli
Aix-Marseille Université
42 PUBLICATIONS **260** CITATIONS
SEE PROFILE

Thierry Chiavassa
Aix-Marseille Université
88 PUBLICATIONS **1,173** CITATIONS
SEE PROFILE

THE JOURNAL OF PHYSICAL CHEMISTRY A

Article

pubs.acs.org/JPCA

Photolysis of Astrophysically Relevant Acrylonitrile: A Matrix Experimental Study

A. Toumi, I. Couturier-Tamburelli,* T. Chiavassa, and N. Piétri*

Aix-Marseille Université, CNRS, PIIM, UMR 7345, 13397 Marseille, France

Supporting Information

ABSTRACT: This report documents the photochemical study of $H_2C{=}C(H)CN$ (acrylonitrile) trapped in low-temperature argon matrices and irradiated with a microwave-discharge hydrogen-flow lamp (λ > 120 nm). We succeeded in identifying $H_2C{=}C(H)NC$ (isoacrylonitrile) as a photoproduct. HC_3N (cyanoacetylene), C_2H_2:HCN (acetylene:hydrogen cyanide), and C_2H_2:HNC (acetylene:hydrogen isocyanide) complexes, which are molecules detected in molecular clouds or in the Titan atmosphere, were also identified. No imine product was observed, but other compounds coming from the HC_3N photolysis have been found. Fourier transform infrared measurements and ^2H substitution experiments coupled with density functional theory calculations (B3LYP/6-31G**) were performed to confirm the spectral assignments of the photochemical products and intermediate species.

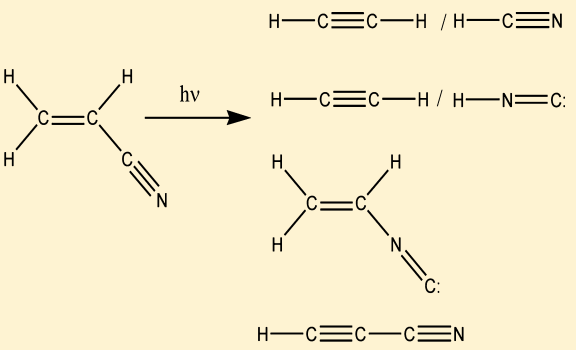

INTRODUCTION

Titan is a solar system object known to possess a massive atmosphere mainly composed of nitrogen and methane.[1] These molecules are subjected to photochemical dissociation by solar UV photons, energetic ions and electrons from Saturn's magnestophere, and cosmic ray particles.[2] These irradiation sources induce a complex chemistry by the reaction of hydrocarbons and nitriles.[3] These reactions create complex molecules and produce the solid organic aerosols responsible for Titan's brownish color.[4] However, the chemical processes that lead to haze formation are poorly understood. Dimitrov and Bar-Nun[5] have suggested that haze is formed in the thermosphere by the absorption of EUV energy, whereas Ferris et al.[6] have suggested that it is produced by solar FUV radiation in the stratosphere. Among the molecules present in the Titan upper atmosphere, a maximum limit has been given for acrylonitrile based on data collected during the Cassini mission.[7,8] Moreover, acrylonitrile is also identified in Titan simulation experiments.[6,9] In the gas phase of planetary atmospheres, the formation of acrylonitrile could result from a fast gas-phase reaction between CN and C_2H_4 or HCN and C_2H_3.[10] Earlier, acrylonitrile was found toward Sgr B_2[11] in the cold, dark cloud TMC-1[12] and in the carbon-rich star IRC +10216.[13]

The mechanisms for atmospheric destruction and more specifically the role of acrylonitrile in Titan's atmosphere are unknown. Therefore, in order to maximize the simulation of the photoreactivity in Titan's gas phase, acrylonitrile is trapped in a rare gas matrix. In this environment, even if the rotation of the molecule is prevented, acrylonitrile is isolated and has a behavior similar to that of a molecule in the gas phase. Nevertheless, the matrix effect may allow us to observe unstable gas-phase species such as complexes or some isomers. To simulate the far UV radiation found in the solar radiation spectrum present in the upper Titan atmosphere, the acrylonitrile is photolyzed with a hydrogen lamp.

Over the last twenty years, the photochemical properties of acrylonitrile have been studied in different conditions.[14−18] The photolysis of acrylonitrile vapor at 213.9 nm was carried out by Gandini and Hackett[12] in 1978. They put into evidence two photochemical channels: an acetylene/hydrogen cyanide channel (ϕ = 0.5) and a cyanoacetylene/hydrogen channel (ϕ = 0.31). Then, the photodissociation of this compound at 193 nm was examined by Blank et al.[15] as well as in argon matrices by Machara et al.[16] These experiments permitted the identification of C_2H_2/HCN and HC_3N. The UV photolysis of acrylonitrile in an N_2 solid environment gave rise to HCN and cyanoacteylene (HC_3N) and may have resulted in isomerizations forming isocyanide or a ketenimine.[17] Later, the photodissociation of this compound and its isotopologue ($CD_2{=}CDCN$) at 193 nm was examined by Wilhelm et al.[18] using time-resolved Fourier transform infrared emission spectroscopy. This study revealed the presence of acetylene, hydrogen cyanide, and its isomer HNC.

In the present study, experimental results are reported on the photochemical decomposition of acrylonitrile trapped in an argon cryogenic matrix at 10 K. This technique allows us to trap intermediates not observed in the gas phase and to provide more details about reaction mechanisms. This work is intended to be an interesting addition to the work of Machara,[16] who has

Received: December 20, 2013
Revised: March 12, 2014

   dx.doi.org/10.1021/jp412481s | J. Phys. Chem. A XXXX, XXX, XXX−XXX

Scheme 1. Supposed Reaction Pathways for the Photolysis Products Obtained by Irradiation of Acrylonitrile at $\lambda > 120$ nm

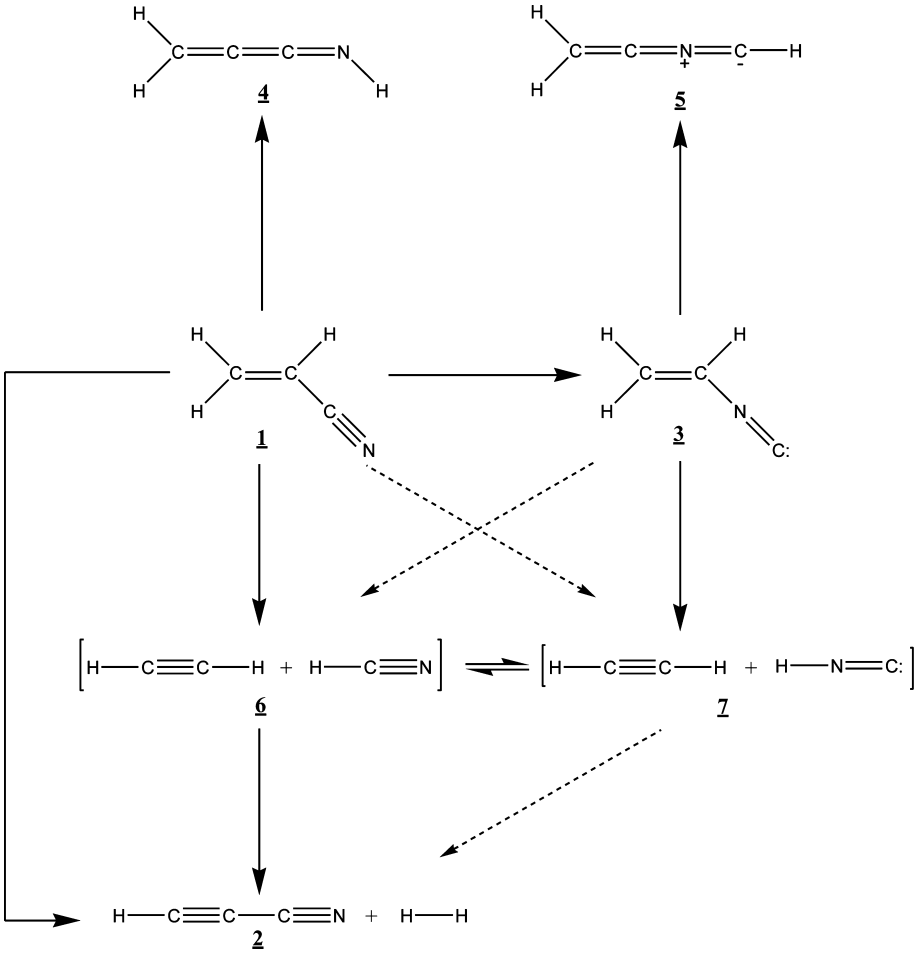

identified only two products of photolysis (HC_3N and C_2H_2/HCN) in argon matrix, leaving many unidentified infrared bands. In regard to all results cited above, we expect the formation of different products illustrated in Scheme 1. In this paper we will discuss the presence of these different compounds, using as support results from isotopomer experiments and theoretical results obtained by Homayoon et al.[19]

EXPERIMENTAL SECTION

Acrylonitrile **1** (from Aldrich ≥99%) and acrylonitrile-D3 (Aldrich, 98 atom % D) **1-D3** were degassed before use. The polymerization of these compounds was not observed in our experiments.

The apparatus and experimental techniques used to obtain the argon matrix have been described elsewhere.[20] The matrix was obtained by spraying a 1/500 mixture of **1** and **1-D3** into argon from a pyrex line onto a golden copper plate cooled at 20 K with the help of a 21 CTI cold head model. The ratios are obtained using standard manometric techniques. The matrix thickness was about 17.8 μm. The spectra were recorded at 10 K in reflection mode using a Fourier transform infrared spectrometer (Nicolet serie II Magna System 750) from 4000 to 650 cm^{-1} using a MCT detector. Each spectrum was averaged over 100 scans and had a 0.12 cm^{-1} resolution.

The samples were irradiated using a microwave discharge hydrogen flow lamp (Opthos instrument) in a range from 120 nm to a continuum in the visible through a MgF_2 window directly connected to our cryostat. The VUV flux in this range of wavelengths was estimated to be around 2×10^{15} photons cm^{-2} s^{-1}.

The vibrational spectra of the reaction products were determined by density functional theory (DFT)[21−23] calculations. The Gaussian 09[24] program package using the B3LYP[25,26] procedure with a 6-31 G** basis set was used for these calculations.

RESULTS

IR Spectroscopy of C_3H_3N and C_3D_3N in Solid Argon. Figure 1 shows the spectra of **1** (top trace) and **1-D3** (bottom trace) trapped in argon matrix at 10 K with a product/Ar ratio of about 1/500. Twelve of the fifteen fundamental vibrational modes have absorption in the 4000−600 cm^{-1} region. The infrared spectrum of acrylonitrile **1** (Cs symmetry) in the gas phase has been studied by different groups.[27−29] Here, we adopt their notations and assignments. The first 11 modes in decreasing order of wavenumber for the A′ vibrational modes are labeled ν_1 to ν_{11}, and the four belonging to the A″ vibrational modes are labeled ν_{12} to ν_{15}. Only absorption bands observed in the 4000−600 cm^{-1} area in argon cryogenic matrix and gaseous phase with their assignments are given in Table 1. The spectrum of acrylonitrile **1** trapped in argon matrix shows narrow bands corresponding to the fundamental and combination modes. Many features are also observed for each mode because different trapping sites can exist in argon matrix for this molecule. The most typical bands are the intense ν_{12} and ν_{13} modes at 974 and 953 cm^{-1}, respectively, and the CN

dx.doi.org/10.1021/jp412481s | J. Phys. Chem. A XXXX, XXX, XXX−XXX

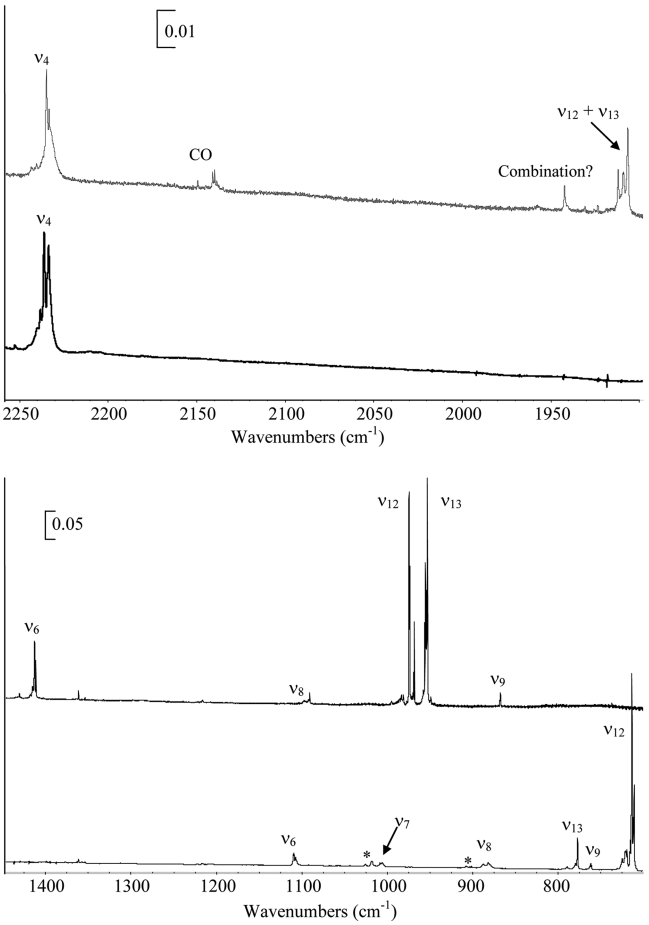

Figure 1. Infrared spectra of acrylonitrile **1** (top) and acrylonitrile D3 **1-D3** (bottom) isolated in argon matrix at 10 K. The bands denoted by an asterisk are assigned to the acrylonitrile D2 compounds.

(ν_4) stretching mode at 2235 cm^{-1}. One band which is not sufficiently intense to be observed in the gas phase, located at 2998 cm^{-1}, is observed. This band can be assigned to combination modes ($\nu_4 + \nu_9$, $\nu_5 + \nu_6$, or $2\nu_{12} + \nu_8$). The spectrum analysis of **1-D3** does not allow us to conclude on the assignment of the combination.

To confirm our assignments we compared the experimental wavenumbers to the theoretical ones calculated with Gaussian 09[24] in the B3LYP method and 6-31G** basis set. Table 1 shows a good agreement between calculated (using a standard scaling factor of 0.96) and experimental wavenumbers and intensities.

The bottom trace of Figure 1 shows the IR spectrum of **1-D3**. When the calculated wavenumbers reported in Table 2 are compared, the fundamental modes can be assigned without ambiguity and some combination modes for this compound can be deduced. Indeed, the theoretical and experimental shifts between **1** and **1-D3** are in very good agreement. However, many bands are observed, namely, at 2236, 1560, 1558, 1025, 1018, 907, and 662 cm^{-1}, which cannot be attributed to **1-D3**. This last compound is synthesized by Aldrich with only 98% atom deuterium. Therefore, we can suppose the presence of C_3HD_2N. A vibrational analysis of this molecule (see Table S1 in Supporting Information) is then performed, which confirms that the bands cited above could be assigned to these species (C_3HD_2N).

Irradiation of Acrylonitrile at λ > 120 nm. When (acrylonitrile) **1**, isolated in matrix, was irradiated at λ > 120 nm in its $\sigma \rightarrow \sigma^*$ (172.5 nm) band, $\pi \rightarrow \pi^*$ (203 nm) and n $\rightarrow$ π^* bands (217 nm),[30−32] a decrease of **1** absorption bands are observed as well as the apparition of new bands in different areas of the spectrum (Figure 2, top trace). The evolution of the integrated absorbance versus time permits us to distinguish some sets of bands.

One of these groups, composed of absorption bands at 3315, 2269, 2076, and 667 cm^{-1}, are easily identified to the cyanoacetylene **2** on the basis of our previous works[33,34] (Table 3). Because **2** is well-known to induce isomerization processes under UV irradiation, we deduce some of their formation. Thus, we have identified the formation of isocyanoacetylene, HC_2NC (3328, 2213, and 2033 cm^{-1}),[35] carbene imine, HNC_3, also called iminopropadienylidene (3562, 2204, and 1906 cm^{-1}),[28,33] and $HCNC_2$ (3276, 2102, and 1920 cm^{-1}).[36] Another set was observed at 2179, 2173, and 1944 cm^{-1}. On the basis of our previous work[37] showing that the C_5N^- anion is an important product of HC_5N photolysis and according to the Kolos et al. work concerning the photochemistry of HC_3N,[38] we can attribute these bands to the C_3N^- anion.

To remove any ambiguity with these assignments, the photolysis of **1-D3** is compared to that of the normal isotopologue (Figure 2, bottom trace). During the isotopic experiment, the formation of DC_3N and its isomers DC_2NC, $DCNC_2$, and the carbene imine DNC_3 are observed (Table 3).

Because the isotopic substitution is not completed and traces of HDCC(D)CN are found during the deposition, the observation of HC_3N during the isotopic photolysis experiment is not surprising (Figure 2, top trace), HDCC(D)CN $\rightarrow$ HC_3N + D_2 (Table S1 of Supporting Information).

Five other bands (2124, 1630, 1116, 918, and 881 cm^{-1}) have the same behavior during the irradiation. This can be seen in the three panels of Figure S1 in Supporting Information which depict the intensities of bands at 1630, 1116, and 918 cm^{-1} plotted as functions of the strongest product band, the one at 2124 cm^{-1} (with correlation factors of 0.99, 0.98, and 0.99, respectively). The bands observed at 2124 and 1630 cm^{-1} are characteristic of νN═C and νC═C stretching modes, respectively (Figure 2). These bands could be attributed to isoacrylonitrile **3** (Table 4). Indeed, the most intense band at 2124 cm^{-1} is close to that observed at 2132 cm^{-1} when acrylonitrile is photolyzed in N_2 solid and which is assigned to the isonitrile CH_2CHNC on the basis of earlier work.[17] However, we irradiated acrylonitrile in nitrogen matrix, presented in Supporting Information (Figure S2), and the same mode for isoacrylonitrile is observed at 2124 cm^{-1}. To confirm this identification, we irradiated **1-D3** at λ > 120 nm and performed harmonic vibrational frequency calculations. The results given in Table 4 show a fairly good accordance between experimental and theoretical frequencies. The comparison between calculated and experimental shifts confirms the formation of isoacrylonitrile, although the stretching CN shift has an opposite sign between the experimental and calculated value. This shift is very small, and the positive or negative sign is not very significant. This isomer is obtained by rotation and recombination of the CN group with the C_2H_3 radical after the break of the CC single bond.

Final product band is found at the frequency 3449 cm^{-1}. This resonance was also observed in Machara's paper[16] but was

dx.doi.org/10.1021/jp412481s | J. Phys. Chem. A XXXX, XXX, XXX−XXX

Table 1. Observed and Simulated Vibrational Frequencies (Scaled with 0.96 Factor) of Acrylonitrile 1

	experiments				theory	
assignment[a]	gas phase wavenumber (cm^{-1})[b]	I	matrix wavenumber (cm^{-1})	I	wavenumber (cm^{-1})	I
ν_1 CH stretch	3133 R				3140	
	3123 Q	4	3124	3		6
	3115 P					
ν_2 CH stretch	3078[c]		3074	14	3063	3
ν_3 CH stretch	3051R					
	3042Q	3	3042	14	3048	1
	3034 P					
combination bands			2998	3		
$\nu_6 + \nu_9$	2290 R					
	2280 Q	2	2277	3		
	2272 P					
ν_4 C≡N stretch	2248 R					
	2240 Q	2	2235	15	2255	23
	2231 P					
$\nu_{12} + \nu_{13}$	1915 R					
	1909 m	13	1907	17		
	1899 P					
$\nu_{12} + \nu_{14}/ \nu_{13} + \nu_{14}$	1661 R					
	1654 Q		1651	<1		
	1645 P					
ν_5 C=C stretch	1623 R					
	1615 Q	11	1616	7	1626	1
	1607 P					
ν_6 CH def	1423 R					
	1415 Q	24	1413	54	1396	20
	1407 P					
ν_7 CH rock	1290 R					
	1281 m		1287	<1	1270	1
	1273 P					
ν_8 CH_2 rock	1103 R					
	1096 Q	8	1097	2	1068	10
	1086 P					
ν_{12} CH_2=C wag	971	100	974	54	968	66
ν_{13} C=CH−CN wag	954	100	953	100	943	100
ν_9 C−C stretch	880 R					
	869 Q	2	867	3	853	3
	861 P					
ν_{14} C=C tors	682 Q	33	683	7	685	36

[a]Ref 28. [b]Ref 29; m: minimum between P and R branches. [c]Ref 27. Experimental and theoretical integrated intensities I are in percentage from the strongest band.

not assigned. This band should be attributed to ν_{NH} of an imine. Interestingly, this feature resembles the strongest and similarly broad IR fundamental band of the analogous imine HNC_3 obtained from cyanoacetylene, where the ν_{NH} is observed at 3562 cm^{-1}.

We performed theoretical calculation for the H_2CCCNH imine **4** (Scheme 1) obtained after 1−3 proton migration from **1** (Table 5). The most intense theoretical infrared band is predicted at 2168 cm^{-1}, and all the bands observed during the experiment in this area come from the HC_3N.[33] The stretching NH mode of **4** calculated at 3295 cm^{-1} (Table 5) has a very small predicted intensity compared to the most intense theoretical infrared band. Moreover, the presence of a 3295 cm^{-1} intense band on our experimental IR spectrum (Figure 2, top trace) cannot suggest the imine **4** formation because if we observe this mode we must observe the most intense one around 2168 cm^{-1}. Therefore, no bands matched those expected by the imine calculation. The results are confirmed by the isotopic **1-D3** experiment.

If we do not observe the imine formation (coming from a 1−3 proton migration) during the photolysis of **1**, it seems possible that we will not be able to observe the 1−3 proton migration from the isoacrylonitrile **3** to form **5**. To confirm this hypothesis, we performed vibrational analysis of **5**. The calculation results show that the most intense infrared band is expected around 1020 cm^{-1}. No bands that are not attributed are observed in this spectrum area, which invalidates the formation of **5** (Table S2 of Supporting Information).

In the fourth group of bands listed in Table 6, those observed at 3281 and 2093 cm^{-1} (Figure 2) could be attributed, in agreement with literature data,[39] to the ν_{CH} mode of C_2H_2 and the ν_{CN} mode of HCN molecule, respectively. The C_2H_2 molecule, trapped in argon matrix, is characterized in infrared by a strong absorption band at 3289 cm^{-1}. The CN stretching modes of HCN[40,41] are observed in argon at 2098 cm^{-1}.

dx.doi.org/10.1021/jp412481s | J. Phys. Chem. A XXXX, XXX, XXX−XXX

Table 2. Observed and Simulated Vibrational Frequencies (Scaled with 0.96 Factor) of Acrylonitrile D3 1-D3[a]

	experiments			theory		
assignment	wavenumber (cm^{-1})	I	$\Delta\nu$	wavenumber (cm^{-1})	I_t	$\Delta\nu$
ν_1	2339	3	−785	2348	4	−792
ν_2	2293	2	–	2281	<4	−782
ν_3	2238	<1	−804	2228	<4	−820
ν_4	2234	12	−1	2253	37	−2
C_3HD_2N	2236	–				
C_3HD_2N	1560	–				
C_3HD_2N	1558	–				
ν_5	1548	<1	−67	1555	<4	−71
$\nu_{12} + \nu_{13}$	1487	4				
$\nu_{13} + \nu_{14}$	1377	<1				
ν_6	1109	6	−304	1093	4	−303
C_3HD_2N	1025	–				
C_3HD_2N	1018	–				
ν_7	1006	6	−281	994	12	−276
C_3HD_2N	907	–				
ν_8	882	6	−215	870	8	−198
ν_{13}	777	13	−176	770	12	−173
ν_9	761	6	−106	745	<4	−108
ν_{12}	713	100	−261	708	100	−260
C_3HD_2N	662	–				
ν_{14}	601	19	−82	605	29	−80

[a] $\Delta\nu$: frequency shifts [ν(**1**) − ν(**1-D3**)]. Experimental and theoretical integrated intensities I are in percentage from the strongest band.

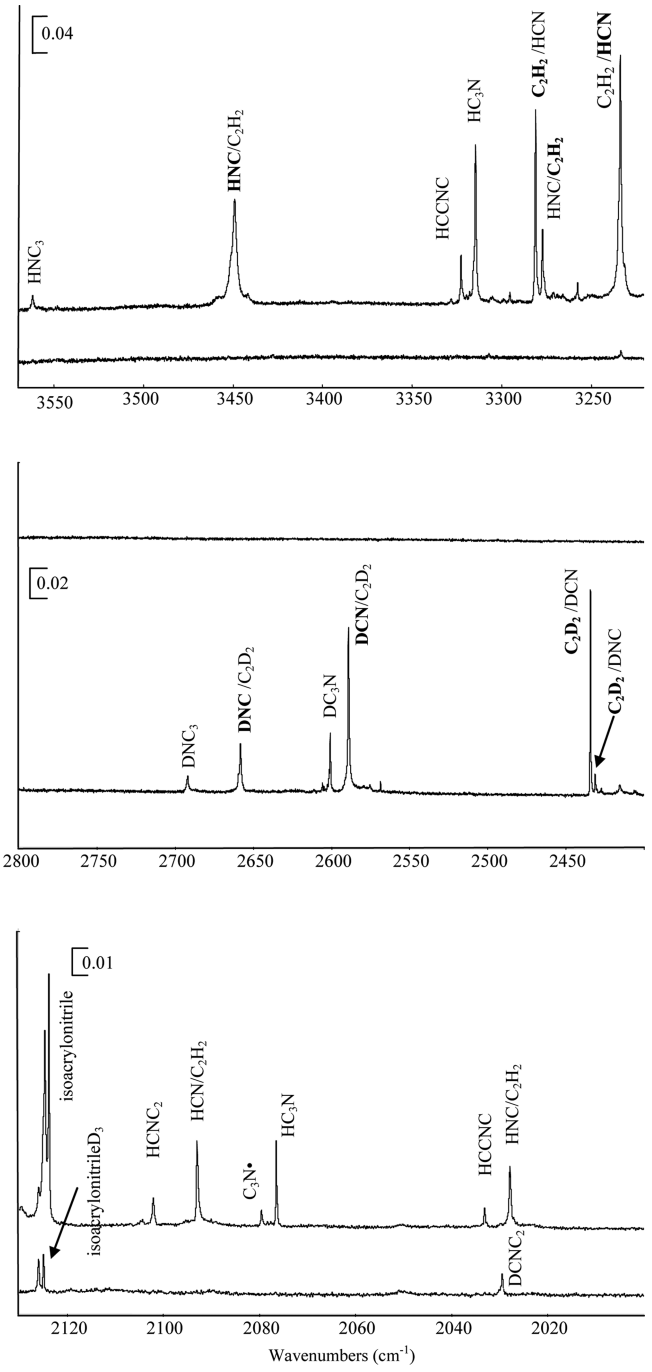

Figure 2. Subtraction spectra (spectrum after 785 min of irradiation spectrum after deposition) of (top trace) acrylonitrile and (bottom trace) acrylonitrile-D3, separately photolyzed at λ > 120 nm in argon matrix at 10 K.

However, in our experiments, the absorption bands observed at 2093 and 3281 cm^{-1} are shifted by 5 and 8 cm^{-1} toward lower frequencies with respect to ν_{CN} mode of HCN monomer and the ν_{CH} mode of acetylene monomer, respectively (Table 6). Therefore, we can assume that these frequency shifts are due to the formation of a complex noted as **6** between the C_2H_2 and HCN trapped in the same cage. The isotopologue experiment confirms this hypothesis, and the results are reported in Table 6. When we performed a C_2H_2/HCN/Ar deposition mixture with a ratio 1/3/1000, we observed, in addition to the bands of monomers, new absorption bands at 3281, 3233, 2092, and 753 cm^{-1} characteristic of the one-to-one association between C_2H_2 and HCN.

In the last group of bands, we observed five bands (Figure 2) at 3449, 3277, 2028, 757, and 740 cm^{-1} (Table 7) assigned, by analogy with the conclusion cited above, to the νHN of HNC[42] molecules, ν_{CH}, ν_{CN}, and δ_{CH} modes of C_2H_2:HNC complex **7**. Indeed, the shifts observed between these vibrational frequencies and those of the monomers in the two isotopomer experiments allow us to conclude a C_2H_2:HNC complex formation (Table 7).

To model the complex structures and their vibrational spectra, theoretical calculations were performed on different starting geometries for each complex (B3LYP/6-31G**). The stabilization energy calculations were described elsewhere in the literature.[43,44] For each energy structure minimum, normal coordinate calculations were done. Calculations yield only two minima. The optimized structures are shown in Scheme 2. The first one, denoted as the L form, exhibits a hydrogen bond between the nitrogen (carbon) atom of HCN (or HNC) and the hydrogen atom of C_2H_2. The second one is the T form, for which hydrogen bonding occurs with the CC triple bond of C_2H_2 and the hydrogen of HCN (HNC). Whatever the structure, the C_2H_2:HCN complex is more stable than the C_2H_2:HNC complex by around 60 kJ/mol. For the two complexes, the T form is more stable than the L form by only 1 and 4.8 kJ/mol (C_2H_2:HCN and C_2H_2:HNC, respectively). After basis set superposition error (BSSE) correction, the T and L forms of the C_2H_2:HCN complex are stabilized with regard to the monomer molecules by 2.9 kJ/mol. For C_2H_2:HNC, the two forms are stabilized with regard to monomers by 5.2 (linear) and 3.4 kJ/mol (T).

The calculated harmonic frequencies of the monomers and those of the complexes C_2H_2:HCN and C_2H_2:HNC are

dx.doi.org/10.1021/jp412481s | J. Phys. Chem. A XXXX, XXX, XXX−XXX

Table 3. Experimental Wavenumbers (cm^{-1}) (B3LYP/6-31G** Scaled with 0.96 Factor) of Cyanoacetylene, Isocyanoacetylene, HNC_3 and $HCNC_2$ and Their D3 Isotopologues

HC_3N		HC_2NC		HNC_3		$HCNC_2$	
Guennoun et al.[33]	this work	Guennoun et al.[33]	this work	Guennoun et al.[33]	this work	Guennoun et al.[33]	this work
3316	3315	3328	3328	3562	3562	3277	3276
2269	2269	2213	2213	2205	2204	2102	2102
2076	2076	2033	2033	1906	1906	1920	1920
667	667						
DC_3N		DC_2NC		DNC_3		$DCNC_2$	
2601	2601	2610	2610	2692	2691	2568	2568
2246	2246	2151	2151	2161	2160	2029	2030
1964	1964	1962	1962	1880	1881		

Table 4. Observed and Simulated Wavenumbers (cm^{-1}) (B3LYP/6-31G** Scaled with 0.96 Factor) of Isoacrylonitrile and Isoacrylonitrile-D3 [$\Delta\nu = \nu$(Isoacrylonitrile)$-\nu$(Isoacrylonitrile-D3)]

	$H_2CC(H)NC$		$D_2CC(D)NC$		$\Delta\nu^a$	
assignment	calc (I)	expt. (I)	calc (I)	expt. (I)	calc	expt.
ν_1 CH stretch	3152 (2)		2357 (1)		795	
ν_2 CH stretch	3071 (3)		2288 (3)		782	
ν_3 CH stretch	3056(<1)		2232 (1)		824	
ν_4 CN stretch	2119(100)	2124 (100)	2118 (100)	2126 (100)	1	−2
ν_5 CC stretch	1634(12)	1630 (9)	1561(11)	1566 (5)	73	64
ν_6 CH def	1385(1)		988 (4)		397	
ν_7 CH def	1285(1)		1094 (5)		191	
ν_8 CH def	1096 (8)	1116 (4)	755 (2)		341	
ν_9 def out of plane	952 (13)	918 (15)	694 (17)	699 (10)	258	219
ν_{10} def out of plane	902 (22)	881(10)	746 (2)	754 (2)	156	127
ν_{11} def in plane	691 (1)		574 (<1)		117	

[a] $\Delta\nu = \nu$(isoacrylonitrile) − ν(isoacrylonitrile-D3).

Table 5. Simulated Wavenumbers (cm^{-1}) (B3LYP/6-31G** Scaled with 0.96 Factor) of Imine and Imine-D3 [$\Delta\nu = \nu$(Imine)$-\nu$(Imine-D3)]

assignment	$H_2C{=}C{=}C{=}NH$	$D_2C{=}C{=}C{=}ND$	$\Delta\nu^a$
νNH (or ND)	3295 (<1)	2424 (9)	871
νCH (or CD)	3050 (3)	2278 (5)	772
νCH (or CD)	2982 (7)	2206 (90)	776
νCC	2168 (100)	2134 (100)	34
νCC	1681 (15)	1646 (38)	35
δCH (or CD)	1415 (2)	1088 (6)	327
δNH (or ND)	1063 (68)	875 (42)	188
δCH (or CD)	1008 (3)	808 (1)	200
δ out of plane	918 (11)	773 (18)	145
	892 (0)	742 (10)	150
δ out of plane	819 (18)	617 (22)	202

[a] $\Delta\nu = \nu$(imine) − ν(imine-D3).

summarized in Tables 6 and 7, respectively. To identify the form existing in argon matrix, with the energy difference between T and L complexes being too weak, we compared the vibrational frequencies of the two complexes with regard to those of the free molecules. Analysis of Tables 6 and 7 shows differences between the calculated frequencies of the T and L complexes. The calculated red shifts for the ν_{HN} (HNC) or ν_{HC} (HCN) stretching modes for the T form are much more important than those obtained for the L form. Indeed, this shift is −4 cm^{-1} for the L-shaped C_2H_2:HCN complex and −77 cm^{-1} for T-shaped, while it is −72 cm^{-1} experimentally. For the C_2H_2:HNC complex, these experimental shifts are −12 and −175 cm^{-1} for the L and T complexes, respectively, while it is −171 cm^{-1} experimentally (Table 7). For the C_2H_2:HCN complex, the ν_{CN} stretching modes of complexed HCN are shifted toward the lower and higher frequencies with respect to the monomer for the T and L forms, respectively (Table 6). In our experiment, this mode is shifted toward lower frequencies by 5 cm^{-1} with respect to the monomers. This fact is in good agreement with the results obtained for the T form. Finally, the shift toward the lower frequencies of the acetylene ν_{CH} for the L form is much more important than those obtained for the T form. Experimentally these shifts are −12 and −8 cm^{-1} for the C_2H_2:HNC and C_2H_2:HCN complexes, respectively. These weak shifts are in agreement with the T values (−10 and −8 respectively). In conclusion, we can say that the two complexes **6** and **7** are formed in the T form.

Discussion. During the Gandini and Hacket[14] experiments, performed at 213.9 nm, only the HCN, C_2H_2, and HC_3N were observed. Later, Wilhelm et al.[18] showed that the dominant molecular elimination channels following the 193 nm dissociation of acrylonitrile resulted in HCN + $:C{=}CH_2$ vinylidene ($^1A_1$) followed closely by the elimination of HNC + acetylene.

Vinylidene in the ($^1A_1$) state was relatively unstable and would quickly be isomerized to acetylene through a low barrier of only a few kilocalories per mole. In this condition acetylene was in a highly rovibrationally state. When acetylene was formed as a coproduct of HNC, no isomerization took place. By examining the corresponding coproduct of acetylene in the 193 nm dissociation reaction, Wilhelm et al.[18] estimated the HCN/HNC branching ratio indirectly. The value obtained for HCN/HNC population ratio was 3.34. Derecskei et al.[45]

dx.doi.org/10.1021/jp412481s | J. Phys. Chem. A XXXX, XXX, XXX−XXX

Table 6. Experimental and Theoretical Frequency Shifts for the C_2H_2:HCN and C_2D_2:DCN Complexes

	experimental			calculation (B3LYP/6-31G**)				
	monomer	complex	$\Delta\nu$	monomer	L	T	$\Delta\nu$ L	$\Delta\nu$ T
C_2H_2	–	–	–	3395	3377	3387	−18	−8
	3289	3281	−8	3299	3264	3291	−35	−8
	1974	–	–	2002	1995	1996	−7	−6
	737	753	16	742	806	757	64	15
HCN	3306	3234	−72	3339	3335	3262	−4	−77
	2098	2093	−5	2125	2133	2118	8	−7
	721	771	50	737	736	798	−1	61
C_2D_2	2701	–	–	2721	2702	2715	−14	−8
	2442	2434	−8	2429	2408	2424	−21	−8
	1760	–	–	1773	1762	1767	−11	−6
		–	–	546	596	558	50	15
DCN	2631	2589	−42	2651	2651	2611	0	−40
	1923	1907	−16	1934	1940	1912	6	−22
	572		–	589	587	642	−2	53

Table 7. Experimental and Theoretical Frequency Shifts for the C_2H_2:HNC and C_2D_2:DNC Complexes

	experimental			calculation (B3LYP/6-31G**)				
	monomer	complex	$\Delta\nu$	monomer	L	T	$\Delta\nu$ L	$\Delta\nu$ T
C_2H_2	–	–	–	3395	3372	3385	−23	−10
	3289	3277	−12	3299	3249	3289	−50	−10
	1974	–	–	2002	1992	1994	−10	−8
	737	757	20	742	851	762	109	20
HNC	3620	3449	−171	3690	3678	3515	−12	−175
	2029	2028	−1	2029	2049	2030	−20	1
C_2D_2	2701	–	–	2721	2703	2713	−18	−8
	2442	2431	−9	2429	2400	2422	−29	−7
	1760	–	–	1773	1758	1765	−15	−8
		–	–	546	630	563	84	16
DNC	2769	2658	−111	2794	2791	2611	−3	−108
	1940			1934	1951	1912	17	−13

performed ab initio calculations for the dissociation channels of acrylonitrile and found two different pathways for HCN formations through three and four-center eliminations. Therefore, the HCN/HNC ratio obtained from their calculations was 124, i.e., HNC formation is negligeable. This value is not in agreement with the experimental value reported above. Therefore, Homayoon et al.[19] conducted a new theoretical study. These calculations provided the seven channels cited below for HCN (HNC) elimination from acrylonitrile, in contrast to only two in previous ab initio calculations.[37] Among the new paths found, the major ones generating HCN or HNC are the formation of these two molecules with acetylene involving, as a first step, the isomerization of acrylonitrile to isoacrylonitrile.

$$\mathbf{1} \rightarrow :CCH_2 + HCN \quad (A)$$

$$\mathbf{1} \rightarrow C_2H_2 + HCN \quad (B)$$

$$\mathbf{1} \rightarrow \mathbf{3} \rightarrow C_2H_2 + HCN \quad (C)$$

$$\mathbf{1} \rightarrow C_2H_2 + HNC \quad (D)$$

$$\mathbf{1} \rightarrow \mathbf{4} \rightarrow :CCH_2 + HNC \quad (E)$$

$$\mathbf{1} \rightarrow \mathbf{3} \rightarrow :CCH_2 + HNC \quad (F)$$

$$\mathbf{1} \rightarrow \mathbf{3} \rightarrow C_2H_2 + HNC \quad (G)$$

These authors are interested in the HCN and HNC relative populations for different acrylonitrile internal energies. This ratio was calculated for three different energies: 120, 148, and 200 kcal/mol.

At the lowest energy of 120 kcal/mol (262 nm), HCN is formed via mechanism A with a probability of 93%. The most important mechanism for the HNC formation is E where the imine **4** is an intermediate. For this energy, the HCN/HNC ratio is 13.7. At 148 kcal/mol (193 nm), the formation of HCN by path A decreases and it is also formed significantly by path B and to a lesser extent by C. HNC is formed primarily through paths F and G. The predicted HCN/HNC branching ratio at 193 nm is 1.9. This ratio becomes 3.3 when it is calculated indirectly from the ratio of rovibrationally excited acetylene over total acetylene, which it is in perfect agreement with the measured experimental values of Wilhem et al.[18]

Finally, at 200 kcal/mol (143 nm), the paths B and G become the dominant channels for the formation of HCN and HNC, respectively. At this energy, the ratio is 1.3, i.e., similar to those found at 148 kcal/mol.

In our experimental conditions (λ > 120 nm and cryogenic matrix), we observed HC_3N and not only both complexes (C_2H_2:HCN and C_2H_2:HNC) but also the isoacrylonitrile. The later compound is probably unstable in gas phase but becomes observable when it is formed in the argon matrix cage. When the CC single bond of acrylonitrile is broken, the CN rotation followed by recombination with C_3H_2 fragment in the argon

dx.doi.org/10.1021/jp412481s | J. Phys. Chem. A XXXX, XXX, XXX−XXX

Scheme 2. Optimized Geometries of C_2H_2:HCN and C_2H_2:HNC Complexes at the B3LYP/6-31g Level of Theory[a]**

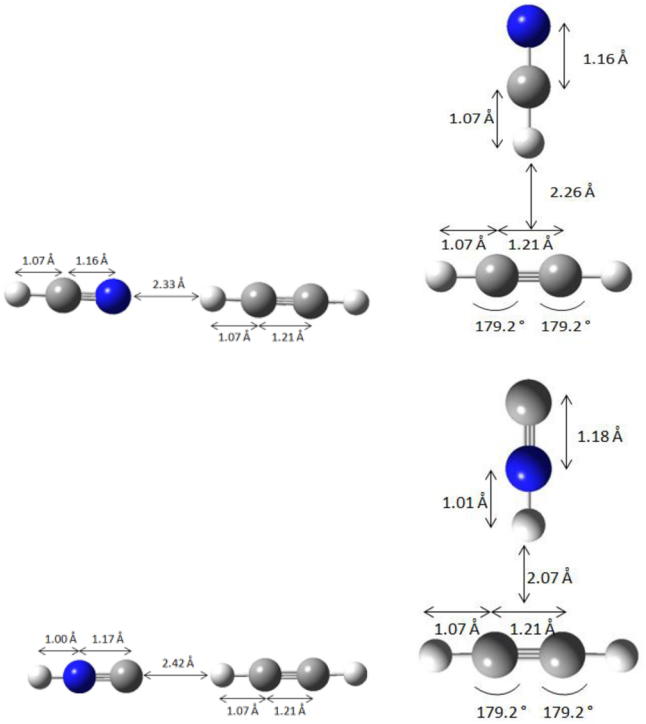

[a]Bond lengths are given in angstroms and angles in degrees.

cage promotes isoacrylonitrile formation. This kind of izomerization process was observed in our previous experiments.[33]

The integrated intensities of several infrared absorption bands were plotted versus irradiation time. We report in Figure 3 the evolution of their most intense absorption bands for

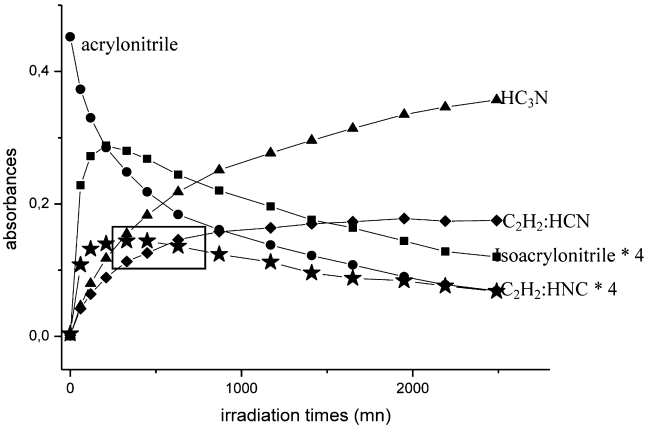

Figure 3. Evolution of integrated absorbances during irradiation at λ > 120 nm of matrix-isolated acrylonitrile at 10 K.

acrylonitrile and its photoproducts. In the very early stage of the acrylonitrile irradiation at λ > 120 nm, the isoacrylonitrile that is formed starts to decrease after 200 min of irradiation. The C_2H_2:HNC complex is also an intermediate product with the maximum of absorbance obtained after 450 min of irradiation. Although these two compounds decrease, we can still see the growing of HC_3N and C_2H_2:HCN complex bands .

The evolution of the HC_3N and C_2H_2:HCN bands versus time shows that these two compounds are formed faster than they are destroyed. Moreover, we have performed the photolysis of mixture HCN/C_2H_2/Ar at λ > 120 nm, and we observe during the irradiation only the formation of the HC_3N, showing that the reaction **1** → **6** is not reversible.

With the hydrogen lamp, acrylonitrile has been irradiated with an atomic hydrogen Lyman α at 120 nm (238 kcal/mol), a broad emission band at 160 nm (180 kcal/mol) generated by molecular hydrogen, and a continuum between 170 and 200 nm (143 < E < 169 kcal/mol). At this irradiation wavelength, the formation of imine **4** is not predicted to be the major process (see path E cited above). Even if we provide sufficient energy to access this intermediate, it will be formed in quantities that are too small to be observed. This result is in good agreement with the fact that the imine is not observed in our experiment. Then we compare our experimental results principally with theoretical ones for 200 and 148 kcal/mol, which show that the HCN is formed with C_2H_2 or :CCH_2 and HNC with C_2H_2 via isoacrylonitrile.

We tried to estimate the HCN/HNC branching ratio to compare this value to that calculated by Homayoon. We measured the ratio of C_2H_2 complexed with HCN to the one complexed with HNC as a function of irradiation time. In the calculation cited above, the author considers that HNC is a final product. In our experiments, it is not the case; we calculated the ratio between the absorbance of the band at 3281 cm^{-1} (ν_{CH} of acetylene in complex C_2H_2:HCN) and those at 3277 cm^{-1} (ν_{CH} of acetylene in complex C_2H_2:HNC) before the decrease of HNC, i.e., between 400 and 900 min of irradiation (see the boxed region of Figure 3). The value obtained is 4.4 ± 0.5.

CONCLUSION

Acrylonitrile has been observed in molecular clouds and in Titan's atmosphere.[7] However, acrylonitrile formation in such environments is likely, and we studied this molecule to determine the reaction products that might be sought on Titan and elsewhere.

The photodissociation of **1** and **1-D3** trapped in argon matrix at 10 K have been performed at 120 nm. This irradiation does not reveal the imine formation but does reveal that of isoacrylonitrile **3** as the first intermediate product. The photodecomposition of this last compound permits the formation of complex C_2H_2:HNC **7**, which isomerizes quickly in the C_2H_2:HCN **6** complex. The large amount of **6** formed shows that this complex comes not only from **7** but also probably from **1**. We have shown that the decomposition of **6** induces the formation of HC_3N. Although this last compound undergoes photoisomerization reactions, it is clearly the final reaction product. The measured HCN/HNC ratio (4.4) is in very good agreement with those of another experiment and calculation,[13] showing that the principal mechanism of formation of HCN is **1** → C_2H_2 and HCN and for HNC is **1** → **3** → C_2H_2 and HNC in our experimental conditions.

ASSOCIATED CONTENT

Supporting Information

Cross correlations of integrated optical densities for four IR absorption bands developed during far UV irradiations of the acrylonitrile trapped in argon matrix assigned to isoacrylonitrile (Figure S1); spectra after 861 min of irradiation and after the deposition when acrylonitrile is photolyzed at λ > 120 nm in N_2 matrix at 10 K (Figure S2); observed and simulated vibrational

dx.doi.org/10.1021/jp412481s | J. Phys. Chem. A XXXX, XXX, XXX−XXX

frequencies of acrylonitrile-D3 and acrylonitrile-D2 (Table S1); simulated vibrational frequencies scaled with 0.96 factor of **5** (Table S2). This material is available free of charge via the Internet at http://pubs.acs.org.

AUTHOR INFORMATION

Corresponding Authors

*E-mail: nathalie.pietri@univ-amu.fr. Tel.: 0033 491288289.
*E-mail: isabelle.couturier@univ-amu.fr.

Notes

The authors declare no competing financial interest.

ACKNOWLEDGMENTS

The theoretical part of this work was conducted using the "Centre Régional de Compétence en Modélisation Moléculaire de Marseille".

REFERENCES

(1) Kuiper, G. P. Titan: A Satellite with an Atmosphere. *Astrophys. J.* **1944**, *100*, 378−383.
(2) Yung, Y. L.; Allen, M.; Pinto, J. P. Photochemistry of the Atmosphere of Titan: Comparison Between Model and Observations. *Astrophys. J. Suppl. Ser.* **1984**, *55*, 465−506.
(3) Vinatier, S.; Bézard, B.; Nixon, C. A.; Mamoutkine, A.; Carlson, R. C.; Jennings, D. E.; Guandique, E. A.; Teanby, N. A.; Bjoraker, G. L.; Flasar, F. M.; et al. Analysis of Cassini/CIRS Limb Spectra of Titan Acquired during the Nominal Mission: I. Hydrocarbon, Nitriles and CO_2 Vertical Mixing Ratio Profiles. *Icarus* **2010**, *205*, 559−570.
(4) Gautier, T.; Carrasco, N.; Buch, A.; Szopa, C.; Sciamma-O'Brien, E.; Cernogora, G. Nitrile Gas Chemistry in Titan's Atmosphere. *Icarus* **2011**, *213*, 625−635.
(5) Dimitrov, B.; Bar-Nun, A. A Model of Energy-Dependent Agglomeration of Hydrocarbon Aerosol Particles and Implication to Titan's Aerosols. *J. Aerosol Sci.* **1999**, *30*, 35−49.
(6) Ferris, J. P.; Tran, B.; Joseph, J.; Vuitton, V.; Briggs, R.; Force, M. The Role of Photochemistry in Titan's Atmospheric Chemistry. *Adv. Space Res.* **2005**, *36*, 251−257.
(7) Cui, J.; Yelle, R. V.; Vuitton, V.; Waite, J. H., Jr; Kasprzak, W. T.; Gell, D. A.; Niemann, H. B.; Müller-Wodarg, I. C. F.; Borggren, N.; Fletcher, G. G.; et al. Analysis of Titan's Neutral Upper Atmosphere from Cassini Ion Neutral Mass Spectrometer Measurements. *Icarus* **2009**, *200*, 581−615.
(8) Lellouch, E.; Vinatier, S.; Moreno, R.; Allen, M.; Gulkis, S.; Hartogh, P.; Krieg, J. M.; Maestrini, A.; Mehdi, I.; Coustenis, A. Sounding of Titan's Atmosphere at Submillimeter Wavelengths from an Orbiting Spacecraft. *Planet. Space Sci.* **2010**, *58*, 1724−1739.
(9) Clarke, D. W.; Joseph, J. C.; Ferris, J. P. The Design and Use of a Photochemical Flow Reactor: A Laboratory Study of the Atmospheric Chemistry of Cyanoacetylene on Titan. *Icarus* **2000**, *147*, 282−291.
(10) Monks, P. S.; Romani, P. N.; Nesbitt, F. L.; Scanlon, M.; Stief, L. J. The Kinetics of the Formation of Nitrile Compounds in the Atmospheres of Titan and Neptune. *J. Geophys. Res.: Planets* **1993**, *98*, 17115−17122.
(11) Gardner, F. F.; Winnewisser, G. The Detection of Interstellar Vinyl Cyanide (Acrylonitrile). *Astrophys. J.* **1975**, *195*, 127−130.
(12) Matthews, H. E.; Sears, T. J. The Detection of Vinyl Cyanide in TMC-1. *Astrophys. J.* **1983**, *272*, 149−153.
(13) Agundez, M.; Cernicharo, J.; Pardo, J. R.; Fonfria Exposito, J. P.; Guélin, M.; Tenenbaum, E. D.; Ziurys, L. M.; Apponi, A. J. Understanding the Chemical Complexity in Circumstellar Envelopes of C-Rich AGB Stars: The Case of IRC +10216. *Astrophys. Space Sci.* **2008**, *313*, 229−233.
(14) Gandini, A.; Hackett, P. A. The Photochemistry of Acrylonitrile Vapour at 213.9 nm. *Can. J. Chem.* **1978**, *56*, 2096−2098.
(15) Blank, D. A.; Swits, A. G.; Lee, Y. T.; North, S. W.; Hall, G. E. Photodissociation of Acrylonitrile at 193 nm: A Photofragment Translational Spectroscopy Study Using Synchrotron Radiation for Product Photoionization. *J. Chem. Phys.* **1998**, *108*, 5784−5794.
(16) Machara, N. P.; Ault, B. S. The 193-nm Excimer Laser Photofragmentation of Alkane and Alkene Nitriles in Argon Matrices. *J. Phys. Chem.* **1988**, *92*, 6241−6245.
(17) Hudson, R. L.; Moore, M. H. Reactions of Nitriles in Ices Relevant to Titan, Comets, and the Interstellar Medium: Formation of Cyanate Ion, Ketenimines, and Isonitriles. *Icarus* **2004**, *172*, 466−478.
(18) Wilhelm, M. J.; Nikow, M.; Letendre, L.; Dai, H. L. Photodissociation of Vinyl Cyanide at 193 nm: Nascent Product Distributions of the Molecular Elimination Channels. *J. Chem. Phys.* **2009**, *130*, 044307.
(19) Homayoon, Z.; Varquez, S. A.; Rodriguez-Fernandez, R.; Martinez-Nunez, E. Ab Initio and RRKM Study of the HCN/HNC Elimination Channels from Vinyl Cyanide. *J. Phys. Chem. A.* **2011**, *115*, 979−985.
(20) Pourcin, J.; Monnier, M.; Verlaque, P.; Davidovics, G.; Lauricella, R.; Colonna, C.; Bodot, H. Site-Selective Infrared Photoisomerization of 2-Fluoroethanol in Low-Temperature Matrices. *J. Mol. Spectrosc.* **1985**, *109*, 186−201.
(21) Hohenberg, P.; Khon, W. Inhomogeneous Electron Gas. *Phys. Rev.* **1964**, *136*, B864−B871.
(22) Kohn, W.; Sham, L. J. Self-Consistent Equations Including Exchange and Correlation Effects. *Phys. Rev.* **1965**, *140*, A1133−A1138.
(23) Koch, W.; Holthausen, M. C. *A Chemist's Guide to Density Theory*; Wiley: Weinheim, Germany, 2002.
(24) Frisch, M. J.; Trucks, M. J.; Schlegel, H. B.; Scuseria, G. E.; Robb, M. A.; Cheeseman, J. R.; Scalmani, G.; Barone, V.; Menucci, B.; Petersson, G. A. et al. *Gaussian 09*, revision A02; Gaussian, Inc: Wallingford, CT, 2009.
(25) Becke, A. D. Density Functional Thermochemistry. III The Role of Exact Exchange. *J. Chem. Phys.* **1993**, *98*, 5648−5652.
(26) Lee, C.; W. Yang, W.; R. G. Parr, R. G. Development of the Colle-Solvetti Correlation-Energy Formula into a Functional of the Electron Density. *Phys. Rev.* **1988**, *B 37*, 785−789.
(27) Halverson, F.; Stamm, R. F.; Whalen, J. J. The Vibrational Spectrum and Thermodynamic Functions of Acrylonitrile. *J. Chem. Phys.* **1948**, *16*, 808−816.
(28) Cerceau, F.; Raulin, F.; Courtin, R.; Gautier, D. Infrared Spectra of Gaseous Mononitriles. Application to the Atmosphere of Titan. *Icarus* **1985**, *62*, 207−220.
(29) Khlifi, M.; Nollet, M.; Paillous, P.; Bruston, P.; Raulin, F.; Bénilan, Y.; Khanna, R. K. Absolute Intesities of the Infrared Bands of Gaseous Acrylonitrile. *J. Mol. Spectrosc.* **1999**, *194*, 206−210.
(30) Müllen, P. A.; Orloff, M. K. The Electronic Spectrum of Acrylonitrile. *Theor. Chim. Acta* **1971**, *23*, 278−284.
(31) Motte-Tollet, F.; Messina, D.; Hubin-Franskin, M. J. Electronic and Vibrational Excitation of Acrylonitrile by Low and Intermediate Energy Electrons. *J. Chem. Phys.* **1995**, *103*, 80−89.
(32) Eden, S.; Limao-Vieira, P.; Kendall, P.; Mason, M. J.; Hoffman, S. V.; Spyrou, S. M. High-Resolution Photoabsorption Studies of Acrylonitrile C_2H_3CN and Acetonitrile CH_3CN. *Eur. Phys. J.* **2003**, *26*, 201−210.
(33) Guennoun, Z.; Couturier-Tamburelli, I.; Piétri, N.; Aycard, J. P. UV Photoisomerisation of Cyano and Dicyanoacetylene: The First Identification of CCNCH and CCCNCN Isomers-Matrix Isolation Infrared and Ab Initio Study. *Chem. Phys. Lett.* **2003**, *368*, 574−583.
(34) Guennoun, Z.; Coupeaud, A.; Couturier-Tamburelli, I.; Piétri, N.; Coussan, S.; Aycard, J. P. Acetylenic/Cyanoacetylenic Complexes: Simulation of the Titan's Atmosphere Chemistry. *Chem. Phys.* **2004**, *300*, 143−151.
(35) Kołos, R.; Waluk, J. Matrix-Isolated Products of Cyanoacetylene Dissociation. *J. Mol. Struct.* **1997**, *408*, 473−476.
(36) Kołos, R.; Sobolewski, A. L. The Infrared Spectroscopy of HNCCC: Matrix Isolation and Density Functional Theory Study. *Chem. Phys. Lett.* **2001**, *344*, 625−630.
(37) Coupeaud, A.; Turowski, M.; Gronowski, M.; Piétri, N.; Couturier-Tamburelli, I.; Kołos, R.; Aycard, J. P. C_5N^- Anion and New

Carbenic Isomers of Cyanodiacetylene: A Matrix Isolation IR Study. *J. Chem. Phys.* **2008**, *128*, 154303.
(38) Kołos, R.; Gronowski, M.; Botschwina, P. Matrix Isolation IR Spectroscopic and Ab Initio Studies of C_3N^- and Related Species. *J. Chem. Phys.* **2008**, *128*, 154305.
(39) Guennoun, Z.; Couturier-Tamburelli, I.; Combes, S.; Aycard, J. P.; Piétri, N. Reaction Path of UV Photolysis of Matrix Isolated Acetyl Cyanide: Formation and Identification of Ketenes, Zwitterion and Keteneimine Intermediates. *J. Phys. Chem. A* **2005**, *109*, 11733−11741.
(40) Satoshi, K.; Takayanagi, M.; Nakata, M. Infrared Spectra of $(HCN)_n$ Clusters in Low-Temperature Argon Matrices. *J. Mol. Struct.* **1997**, *413*, 365−369.
(41) King, C. M.; Nixon, E. R. Matrix-Isolation Study of the Hydrogen Cyanide Dimer. *J. Chem. Phys.* **1968**, *48*, 1685−1696.
(42) Milligan, D. E.; Jacox, M. E. Spectroscopic Study of the Vacuum-Ultraviolet Photoplysis of Matrix-Isolation HCN and Halogen Cyanides. Infrared Spectra of the Species CN and XNC. *J. Chem. Phys.* **1967**, *47*, 278−286.
(43) Piétri, N.; Tamburelli, I.; Allouche, A.; Aycard, J. P.; Chiavassa, T. FT-IR Spectra and Photoreactivity of the C_3O_2:HCl Complex Isolated in Solid Argon. *J. Mol. Struct.* **1997**, *416*, 187−195.
(44) Coupeaud, A.; Piétri, N.; Aycard, J. P.; Couturier-Tamburelli, I. Water/Cyanobutadiyne Complexes: An Infrared Matrix Isolation and Theoretical Study. *Phys. Chem. Chem. Phys.* **2007**, *9*, 3985−3991.
(45) Derecskei-Kovacs, A.; North, S. W. The Unimolecular Dissociation of Vinylcyanide: A Theoretical Investigation of a Complex Multichannel Reaction. *J. Chem. Phys.* **1999**, *110*, 2862−2871.